ORIGINAL RESEARCH ■ GASTROINTESTINAL IMAGING

Radiology

Can Current Preoperative Imaging Be Used to Detect Microvascular Invasion of Hepatocellular Carcinoma?[1]

Matteo Renzulli, MD
Stefano Brocchi, MD
Alessandro Cucchetti, MD
Federico Mazzotti, MD
Cristina Mosconi, MD
Camilla Sportoletti, MD
Giovanni Brandi, MD
Antonio Daniele Pinna, MD
Rita Golfieri, MD

Purpose: To determine the accuracy of imaging features, such as tumor dimension, multinodularity, nonsmooth tumor margins, peritumoral enhancement, and radiogenomic algorithm based on the association between imaging features (internal arteries and hypoattenuating halos) and gene expression that the authors called two-trait predictor of venous invasion (TTPVI), in the prediction of microvascular invasion (MVI) in hepatocellular carcinoma (HCC).

Materials and Methods: This single-center retrospective study was approved by the institutional review board, and the requirement for informed consent was waived. One hundred twenty-five patients (median age, 63 years; interquartile range, 53–71 years) with a diagnosis of HCC and indications for hepatic resection were included. Two observers independently reviewed radiologic images to evaluate the following features for MVI: maximum diameter, number of lesions, tumor margins, TTPVI, and peritumoral enhancement. Interobserver agreement was checked, and diagnostic accuracy of radiologic features was investigated.

Results: The total number of HCC nodules was 140. Large tumor size, nonsmooth tumor margins, TTPVI, and peritumoral enhancement were significantly related to the presence of MVI ($P < .05$ in all cases and for both observers). Multinodularity was not significantly related ($P = .158$). Moreover, the diagnostic accuracy of the three "worrisome" radiologic features (nonsmooth tumor margins, peritumoral enhancement, and TTPVI) was associated with tumor size: The negative predictive value of the absence of worrisome features decreased from 0.84 for observer 1 and 0.91 for observer 2 for tumors smaller than 2 cm to 0.56 and 0.71, respectively, for tumors larger than 5 cm, whereas the presence of all three worrisome features returned to a positive predictive value of 0.95 for observer 1 and 0.96 for observer 2 independent of tumor size, with no significant interobserver differences ($P > .10$).

Conclusion: "Worrisome" imaging features, such as tumor dimension, nonsmooth tumor margins, peritumoral enhancement, and TTPVI, have high accuracy in the prediction of MVI in HCC.

©RSNA, 2015

Online supplemental material is available for this article.

Hepatocellular carcinoma (HCC) represents a global health problem because it is the third leading cause of cancer-related deaths worldwide, with an incidence-to-mortality ratio close to 1.0 (1).

One of the greatest problems plaguing the curative treatments of HCC is the unsatisfactory overall survival, due to the high rate of recurrence (2,3). Five-year HCC recurrence complicates 25% of cases after liver transplantation and 70% of cases after hepatic resection (3,4).

Vascular invasion is repeatedly identified as a predictor of recurrence and poor overall survival (2,5). Macrovascular invasion and microvascular invasion (MVI) of HCC are related to a 15- and 4.4-fold increased risk of tumor recurrence, respectively (6). However, in contrast to macrovascular invasion, MVI is difficult to detect with the preoperative imaging techniques recommended for HCC diagnosis and staging by the American Association for the Study of Liver Diseases (AASLD) guidelines, such as computed tomography (CT) or magnetic resonance (MR) imaging (1,7,8). Moreover, the detection of MVI by using preoperative biopsy has proven unreliable because of the intratumoral heterogeneity that causes sampling error (9). MVI is diagnosed only after surgical treatments by means of histopathologic evaluation. Therefore, owing to its late postoperative diagnosis, MVI has limited usefulness in current clinical practice because HCC treatment decisions are usually based on clinical and imaging findings alone (1).

MVI is one of the most important predictors of early recurrence, the so-called true recurrence, arising within the first 2 years after curative treatments (4). After liver transplantation, MVI positivity shortens the disease-free survival at 3 years (relative risk, 3.41) and overall survival at 3 and 5 years (relative risk, 2.41 and 2.29, respectively) and, also after hepatic resection, MVI positivity affects disease-free survival at 3 and 5 years (relative risk, 1.82 and 1.51, respectively) (10).

A future preoperative prediction of MVI would allow appropriate patient selection for both liver transplantation and hepatic resection (11–16).

Tumor characteristics (dimension and multinodularity) (11,17); imaging features, such as nonsmooth tumor margins and peritumoral enhancement (18,19); and radiogenomic algorithm based on the association between imaging features (internal arteries and hypoattenuating halos) and gene expression that we called two-trait predictor of venous invasion (TTPVI) (20) have previously been suggested as predictors of MVI. However, to date, these criteria for a preoperative radiologic diagnosis of MVI in HCC have not been widely recognized (1,11).

The purpose of this study was to determine the accuracy of imaging features, such as tumor dimension, multinodularity, nonsmooth tumor margins, peritumoral enhancement, and TTPVI, in the prediction of MVI in HCC.

Materials and Methods

Patients and Methods

This single-center retrospective study, performed at our tertiary liver care center, was approved by the institutional review board, and the requirement for informed consent was waived.

The surgical database was reviewed from January 2008 to December 2013

Advances in Knowledge

- Some "worrisome" imaging features, such as large tumor size, nonsmooth tumor margins, peritumoral enhancement, and radiogenomic algorithm (based on the association between imaging features [internal arteries and hypoattenuating halos] and gene expression that we called two-trait predictor of venous invasion [TTPVI]) were used to significantly predict the presence of microvascular invasion (MVI) in hepatocellular carcinoma (HCC) ($P < .05$ in all cases and for both observers).

- The identification of the three "worrisome" radiologic features—nonsmooth tumor margins, peritumoral enhancement, and TTPVI—has a high positive predictive value (0.95 for observer 1 and 0.96 for observer 2) in the prediction of MVI in HCC, independent of tumor size, with no significant difference between the areas under the receiver operating characteristic curves of the two observers in the three size groups: $P = .111$ for tumors smaller than 2 cm, $P = .176$ for tumors 2–5 cm, and $P = .368$ for tumors larger than 5 cm.

Implication for Patient Care

- The simultaneous nodule positivity with the three "worrisome" radiologic features (nonsmooth tumor margins, peritumoral enhancement, and TTPVI), regardless tumor size, might play an important role in the present and future management of HCC by allowing the identification of patients with MVI during the decision-making stage.

to identify all patients who underwent hepatic resection for HCC at the Surgical Unit of the Department of Medical and Surgical Sciences–DIMEC of the Sant'Orsola-Malpighi University Hospital of Bologna, Bologna, Italy.

The patients that satisfied the following criteria were included in our study: *(a)* preoperative imaging (CT or MR imaging) was performed in our radiology unit, *(b)* an HCC imaging diagnosis was reached according to the AASLD guidelines until 2010 (21) and according to to their updated versions until 2013 (1,22), and *(c)* hepatic resection was indicated according to the criteria described in a previously published article (23). Patients with previous local-regional treatments or those who received treatment during the period between CT or MR imaging and hepatic resection were excluded.

In the study period, 230 patients with HCC were submitted for surgery. Of these, 20 who received previous treatments, 75 who had preoperative imaging performed outside our radiology unit, and 10 who had inadequate imaging studies were excluded, thus allowing the analysis in 125 patients.

Our protocol requirements for contrast material–enhanced CT and MR imaging have met the criteria recommended by the AASLD guideline (21,22). The technical specifications of CT and MR imaging are explained in Appendix E1 (online).

Image Analysis

All CT and MR images were retrieved from our institutional picture archiving and communication system (Carestream PACS, version 1.1; Kodak, Rochester, NY).

The images were assessed by two radiologists with 5 (S.B.) and 14 (M.R.) years of experience in hepatic imaging, who were aware that the patients had HCC but were blinded to all of the other information, including clinical history, imaging report, and pathologic findings concerning MVI. The two observers independently reviewed all radiologic images

to evaluate the following features for MVI in each individual lesion: *(a)* A maximum diameter larger than 5 cm was noted (17). The precise dimensions of all nodules were collected and classified into three size groups (<2 cm, 2–5 cm, and >5 cm). *(b)* The number of lesions was assessed (11). The number of HCCs identified during radiologic assessment was classified into three main groups according to Vitale et al (24): single, oligonodular (two or three nodules), or multinodular (more than three nodules). *(c)* We analyzed the tumor margins of all nodules to identify the nodules with smooth margins (defined as nodular tumors in all imaging planes) and those with nonsmooth margins (defined as nonnodular tumors in all imaging planes) (18,19). The nonsmooth margins, suggested as a predictor of MVI, were also categorized in the case of focal extranodular extension, crescent extranodular extension beyond the tumor capsule, multinodular confluence appearance, and focal infiltrative margin, respectively (Fig 1). *(d)* TTPVI was assessed (20) and consisted of the identification of two separate CT features (the presence of internal arteries and hypoattenuating halos) that can help predict MVI according to the algorithm detailed in Figure 2, *A*. *(e)* Peritumoral enhancement was defined as the existence of a detectable portion enhancing in the arterial phase, adjacent to the tumor border, later becoming isoattenuating on CT images or isointense on MR images as compared with the background liver parenchyma in the equilibrium phase (Fig 3) (18,19).

Each individual nodule was evaluated on all sections by using different planes (axial, coronal, and sagittal) to assess maximum diameter, tumor margins, TTPVI, and peritumoral enhancement.

All data were collected in a shared database.

Histopathologic Analysis

At our hospital, the presence or absence of MVI is always described in postoperative pathologic reports, which therefore

was the reference standard for MVI of HCC. All pathologic examinations were performed by a team of pathologists, each one with more than 10 years of experience in liver pathology. MVI was defined as a tumor within a vascular space lined by endothelium, which was visible only at microscopy (5). The MVI of tumor cells into the portal or hepatic venules and capillaries was pathologically examined by sampling the HCC tissue. For HCCs up to 5 cm, the entire tumor was examined. For larger tumors, more than 70% of the HCC border was sampled to include the regions suspicious for vascular invasion at gross examination and was evaluated microscopically. The presence of cirrhosis was also evaluated in surgical specimens.

Statistical Analysis

Categorical variables are reported as the number of cases and percentages, and differences between the subgroups were compared by using the Fisher exact test. The distribution of the continuous variables was first checked for normality by using the Kolmogorov-Smirnov test. Since a normal distribution could not be confirmed for most variables, continuous variables were reported as medians and interquartile ranges (except for patient age for descriptive purposes), and the differences between the subgroups were compared by using the Mann-Whitney test. Interobserver agreement was checked by using the Cohen κ statistic; agreement was considered excellent if κ was more than 0.80, good if κ ranged from 0.61 to 0.80, moderate if κ ranged from 0.41 to 0.60, and poor if it was 0.40 or less. The diagnostic accuracy of the radiologic features was investigated by measuring the positive and negative predictive values, as well as the area under the receiver operating characteristic curve (AUROC). All the analyses were performed by using Stata software (StataCorp, College Station, Tex). A P value less than .05 was considered to indicate a statistically significant difference in all analyses.
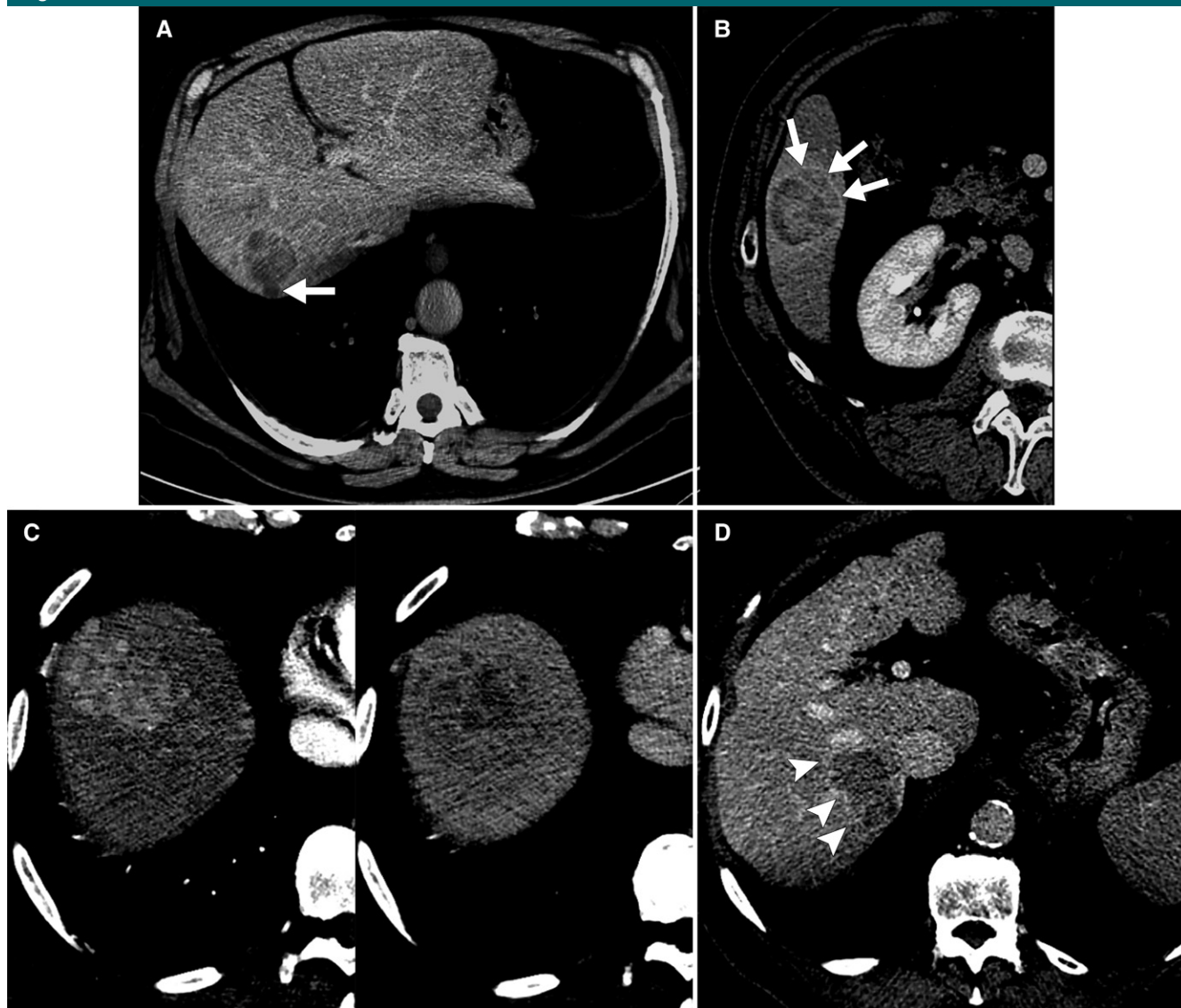
Figure 1

Figure 1: Axial CT images show a nonsmooth tumor margin, suggestive of MVI. *A*, Focal extranodular extension (arrow) in the delayed phase. *B*, Crescent extranodular extension beyond the tumor capsule (arrows) in the delayed phase. *C*, Multinodular confluent appearance in the arterial phase (left) and in the delayed phase (right). *D*, Tumor with focal infiltrative margin (arrowheads) in the delayed phase.

Results

The baseline characteristics of the study population are reported in Table 1. There were 144 tumors in 125 patients. Preoperative imaging in 117 patients was accomplished with CT scanning and in 27 with MR imaging. Of the 144 tumors detected, four were multinodular HCC and were deemed not resectable at the time of surgery; they were intraoperatively ablated. Thus, the total number of resected HCC lesions, for which both radiologic preoperative assessment and pathologic findings were available, was 140 in 125 patients.

Imaging Features of MVI

Of the 140 HCCs, 114 nodules were diagnosed at CT and 26 at MR imaging (Table 2). Overall, nonsmooth tumor margins were present in 55% of HCCs for observer 1 (77 of 140 nodules) and in 59.3% of HCCs for observer 2 (83 of 140 nodules). A focal infiltrative margin was the most frequently diagnosed feature in 25.7% of nodules (36 of 140) for observer 1 and in 26.4% of nodules (37 of 140) for observer 2. TTPVI was present in 57.8% of nodules (81 of 140) for observer 1 and in 57.1% of nodules (80 of 140)
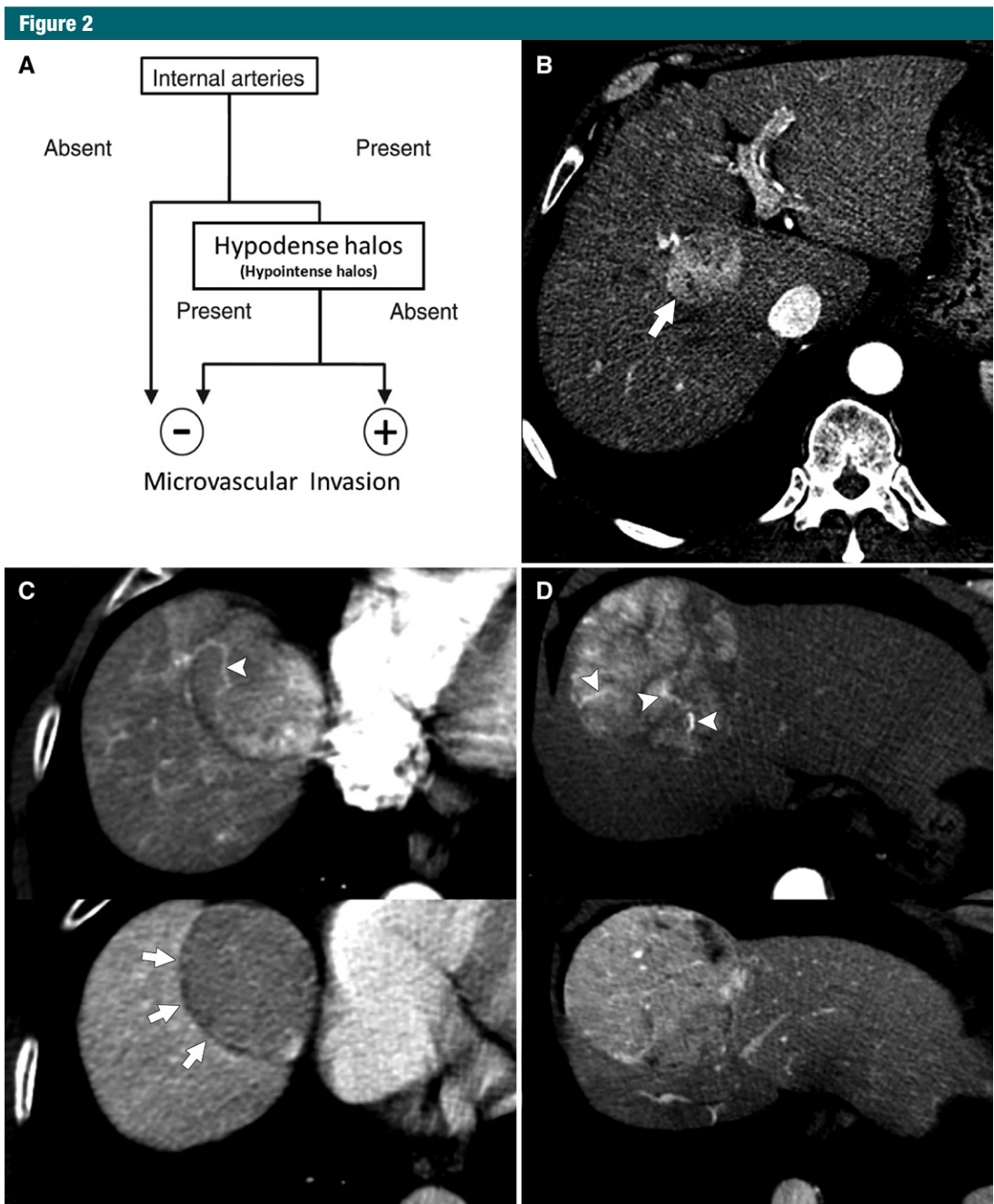
Figure 2: TTPVI. *A,* The two-trait algorithm predictive of MVI, modified from Segal et al (20), is based on the imaging identification of two features: internal arteries assessed in the arterial phase and hypoattenuating halos at CT (or hypointense halos at MR imaging) evaluated in the portal venous or equilibrium phases. *B–D,* Axial CT images show the three possible combinations of these two imaging features. *B,* Homogeneously hyperattenuating tumor (arrow) is seen without appreciable internal arteries, suggestive of the absence of MVI. *C,* Tumor with internal arteries (arrowhead on the upper image) and continuous hypoattenuating halos (arrows on the lower image) is indicative of the absence of MVI. *D,* Tumor with internal arteries (arrowheads on the upper image) and noncontinuous hypoattenuating halos (lower image) is suggestive of MVI.

for observer 2. Peritumoral enhancement was present in 47.1% of nodules (66 of 140) for observer 1 and in 41.4% of nodules (58 of 140) for observer 2. Even if slightly different observations were reached, agreement between the two observers was more than 0.80 for all features considered (Table 2).
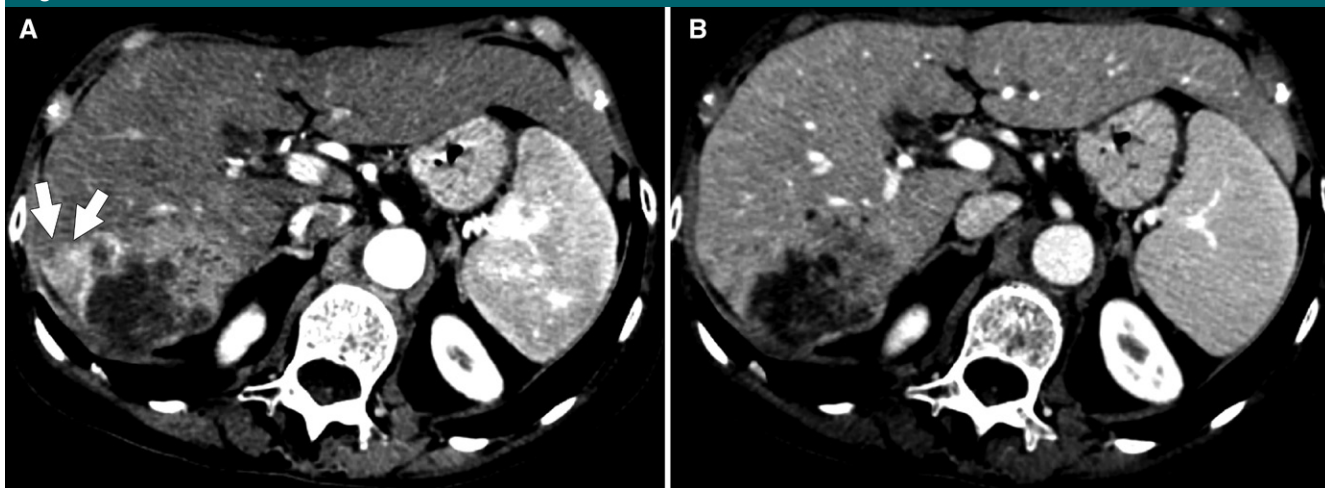
Figure 3

Figure 3: Axial CT images show peritumoral enhancement. *A,* External portion enhancing in the arterial phase in the lateral aspect (arrows), *B,* appears isoattenuating when compared with the background parenchyma in the equilibrium phase.

Indicators of MVI

MVI was present at pathologic examination in 90 of 140 nodules (64.3%). As reported in Table 3, larger tumor size, the presence of nonsmooth tumor margins (Fig 1, *B–E*), TTPVI (Fig 2, *B–D*), and peritumoral enhancement (Fig 3) were significantly related to the presence of MVI. In particular, in the presence of nonsmooth tumor margins, the prevalence of MVI was 76.7% (69 of 90 nodules) and 83.3% (75 of 90 nodules) for observers 1 and 2, respectively ($P < .001$ for both observers). In the presence of TTPVI, the prevalence of MVI was 81.1% (73 of 90 nodules) and 82.2% (74 of 90 nodules) for observers 1 and 2, respectively ($P < .001$ for both). In the presence of peritumoral enhancement, the prevalence of MVI was 65.6% (59 of 90 nodules) and 58.9% (53 of 90 nodules) for observers 1 and 2, respectively ($P < .001$ for both). Of note, within the nonsmooth tumor margins, the focal infiltrative aspect was the radiologic pattern most closely associated with MVI ($P < .001$ for both observers), whereas the presence of mixed features was not found to be associated with MVI ($P = .259$ and $P = .421$ for observers 1 and 2, respectively). Even if a slightly higher prevalence of MVI was observed in the presence of multiple HCCs, multinodularity was not found to be significantly related to MVI ($P = .158$).

Accuracy Statistics for MVI Prediction

Overall, for observer 1, 52 of 140 nodules (37.1%) had no "worrisome" radiologic features, 12 of 140 (8.6%) had one worrisome feature, 16 of 140 (11.4%) had two worrisome features, and 60 of 140 (42.8%) had three worrisome features. The corresponding figures for observer 2 were as follows: 45 of 140 nodules (32.1%), 22 of 140 nodules (15.7%), 20 of 140 nodules (14.3%), and 53 of 140 nodules (37.8%), respectively. The worrisome features were grouped into none (52 and 45 nodules for observers 1 and 2, respectively), one or two (28 and 42 nodules, respectively), and three (60 and 53 nodules, respectively) for the accuracy statistics. AUROCs of each radiologic feature and the sum of features are reported in Figure 4. As can be noted, the combination of the presence of nonsmooth tumor margins, TTPVI, and peritumoral enhancement returned higher AUROC values than did each single radiologic feature. The diagnostic accuracy of the "worrisome" radiologic features was found to be a function of tumor size (Table 4). The negative predictive value of the absence of worrisome features decreased from 0.84 for observer 1 and 0.91 for observer 2 for tumors smaller than 2 cm to 0.56 and 0.71, respectively, for tumors larger than 5 cm, whereas the presence of all three radiologic features always returned to a positive predictive value above 0.90, independent of tumor size.

Considering all the 140 tumors, the AUROC of observer 2 was significantly higher than that of observer 1 ($P = .015$), but no significant difference was observed between the AUROCs of the two observers in the three size groups ($P = .111$ for tumors smaller than 2 cm, $P = .176$ for tumors 2–5 cm, and $P = 0.368$ for tumors larger than 5 cm), because of the smaller sample size in the subgroups.

Discussion

In our study, we assessed the accuracy of different "worrisome" radiologic features in the prediction of MVI in a larger number of nodules than that in previous studies (11,17–20), with MVI identified in 64% of nodules (90 of 140) detected at pathologic examination. Our results demonstrated that nonsmooth tumor margins, peritumoral enhancement, TTPVI, and large tumor size were significantly related to MVI, with good interobserver agreement.

Table 1

Baseline Characteristics of the Study Population

Variable	Value
Age (y)*	63 (53–71)
Mean (y)[†]	62.4 ± 11.2
Male sex	101 (80.8)
Age (y)*	61 (53–71)
Mean age (y)[†]	61.9 ± 10.5
Female sex	24 (19.2)
Age (y)*	66 (59–75)
Mean age (y)[†]	64.5 ± 14.0
Hepatitis C infection	78 (62.4)
Hepatitis B infection	22 (17.6)
Other disease origins	29 (23.2)
Total bilirubin level (mg/dL)	0.75 (0.58–0.95)
Serum albumin level (g/dL)	4.0 (3.5–4.3)
Serum creatinine level (mg/dL)	0.83 (0.75–0.96)
International normalized ratio	1.14 (1.08–1.22)
Platelet count ($\times10^3$/μL)	133 (94–184)
Model for End-Stage Liver Disease score	8 (8–9)
Child–Pugh class	
Class 5	90 (72.0)
Class 6	27 (21.6)
Class 7	8 (6.4)
Presence of cirrhosis	87 (69.6)
Maximum diameter of largest tumor (cm)	3.3 (1.8–5.2)
Largest diameter > 5 cm	42 (30.0)
No. of tumors	
Solitary tumor	113 (90.4)
Two tumors	10 (8.0)
Three tumors	1 (0.8)
Four tumors	1 (0.8)
Extension of hepatectomy	
Single or multiple wedges	69 (55.2)
Segmentectomy	26 (20.8)
Bisegmentectomy	7 (5.6)
Major hepatectomy	23 (18.4)

Note.—Unless indicated otherwise, data are number of patients, with percentages in parentheses. The total number of patients was 125. The total number of tumors was 140; of these, 114 were investigated with CT and 26 with MR imaging. To convert milligrams per deciliter to micromoles per liter for total bilirubin level, multiply by 17.104. To convert milligrams per deciliter to micromoles per liter for serum creatinine level, multiply by 88.4. To convert $\times10^3$/μL to $\times10^9$/L, multiply by 1.0.

* Data are continuous variables, reported as medians with interquartile ranges in parentheses (25th–75th percentiles).

[†] Data are means ± standard deviations.

Table 2

Radiologic Features of 140 HCCs and Agreement between Observers

Parameter	Observer 1	Observer 2	Cohen Agreement (κ values)
All HCCs (140 lesions)			
Maximum tumor diameter (mm)*	33 (18–52)	33 (18–52)	…
Nonsmooth tumor margin			0.825
Yes	77	83	
No	63	57	
Focal extranodular extension	10 (7.1)	15 (10.7)	0.694
Crescent extranodular extension beyond the tumor capsule	12 (8.6)	10 (7.1)	0.803
Multinodular confluence appearance	11 (7.8)	14 (10.0)	0.868
Focal infiltrative margins	36 (25.7)	37 (26.4)	0.907
Mixed features	8 (5.7)	7 (5.0)	0.789
TTPVI			0.898
Present	81	80	
Absent	59	60	
Irregular circumferential peritumoral enhancement			0.885
Present	66	58	
Absent	74	82	
CT examination (114 nodules)			
Maximum tumor diameter (mm)*	34 (20–53)	34 (20–53)	…
Nonsmooth tumor margin			0.813
Yes	68	76	
No	46	38	
TTPVI			0.905
Present	74	71	
Absent	40	43	
Irregular circumferential peritumoral enhancement			0.895
Present	59	53	
Absent	55	61	
MR imaging (26 nodules)			
Maximum tumor diameter (mm)*	22 (14–43)	22 (14–43)	…
Nonsmooth tumor margin			0.821
Yes	9	7	
No	17	19	
TTPVI			0.821
Present	7	9	
Absent	19	17	
Irregular circumferential peritumoral enhancement			0.785
Present	7	5	
Absent	19	21	

Note.—Unless indicated otherwise, data are number of tumors, with percentages in parentheses. Interobserver agreement was considered excellent if κ was more than 0.80, good if κ ranged from 0.61 to 0.80, moderate if κ ranged from 0.41 to 0.60, and poor if κ was 0.40 or less. MVI was observed in 90 of 140 HCCs (64.3%).

* Data are continuous variables, reported as medians with interquartile ranges in parentheses (25th–75th percentiles).

Previously, "single nodule type with extranodular growth" and "confluent multinodular type" have been reported as important predictors of MVI pathologically and showed higher frequencies of vessel invasion than the "single nodular type" (17).

In our study, the presence of nonsmooth tumor margins was highly predictive of histologic MVI; among the different types of nonsmooth tumor margins, the focal infiltrative aspect (Fig 1, *D*) was the radiologic pattern most closely associated with MVI ($P < .001$ for both

observers). This figure was similar to what had previously been reported by Chou et al (18,19) in which MVI most frequently occurred at the site of extranodular extension, which was categorized differently by those authors into the focal or multifocal outgrowth of nodules protruding into the nontumor parenchyma, without mention of the infiltrative type. We hypothesize that MVI might occur when tumor margins are invaded, regardless of the infiltrative or extranodular growth outlines assessable with imaging.

Peritumoral enhancement was an additional significant marker of histologic MVI ($P < .001$), in good agreement with the results of previous studies (6,25,26). This probably relates to the known hypothesis of hemodynamic perfusion changes existing in compensatory arterial hyperperfusion, which can occur in the area of decreased portal flow because of the minute portal branch occlusion caused by tumor thrombi, assuming that the draining veins of encapsulated HCCs are usually portal venules (27). Kim et al (25) have described the same pattern detected at gadolinium ethoxybenzyl diethylenetriamine pentaacetic acid MR imaging, including hepatobiliary phase images, as a risk factor for MVI. Miyata et al (6), using CT hepatic arteriography, have demonstrated that the distortion of the coronal enhancement and the tumor arterioportal shunt could be significant predictors of portal vein tumor invasion, and Nishie et al (26) have proven that the size of peritumoral enhancement was a significant risk factor for MVI detected

Table 3

Radiologic Features of HCC and Relationship with MVI

Parameter	MVI Absent ($n = 50$)	MVI Present ($n = 90$)	P Value
General tumor features			
Largest diameter (mm)*	19 (14–35)	41 (24–57)	<.001
<2 cm	25/37 (67.6)	12/37 (32.4)	
2–5 cm	18/62 (29.0)	44/62 (71.0)	
>5 cm	7/41 (17.1)	34/41 (82.9)	
Presence of multiple nodules	1 (2.0)	8 (8.9)	.158
Observer 1			
Nonsmooth tumor margin	8 (16.0)	69 (76.7)	<.001
Focal extranodular extension	1 (2.0)	9 (10.0)	.096
Extension beyond the tumor capsule	1 (2.0)	11 (12.2)	.056
Multinodular confluence appearance	1 (2.0)	10 (11.1)	.097
Focal infiltrative margins	4 (8.0)	32 (35.6)	<.001
Mixed features	1 (2.0)	7 (7.8)	.259
TTPVI present	8 (16.0)	73 (81.1)	<.001
Irregular peritumoral enhancement present	7 (14.0)	59 (65.6)	<.001
Observer 2			
Nonsmooth tumor margin	8 (16.0)	75 (83.3)	<.001
Focal extranodular extension	2 (4.0)	13 (14.4)	.085
Extension beyond the tumor capsule	0 (0.0)	10 (11.1)	.014
Multinodular confluence appearance	1 (2.0)	13 (14.4)	.019
Focal infiltrative margins	4 (8.0)	33 (36.7)	<.001
Mixed features	1 (2.0)	6 (6.7)	.421
TTPVI present	6 (12.0)	74 (82.2)	<.001
Irregular peritumoral enhancement present	5 (10.0)	53 (58.9)	<.001

Note.—Unless indicated otherwise, data are number of tumors, with percentages in parentheses. Categorical variables were compared by using the Fisher exact test.

* Data are continuous variables, reported as medians with interquartile ranges in parentheses (25th–75th percentiles), and were compared by using the Mann-Whitney test.
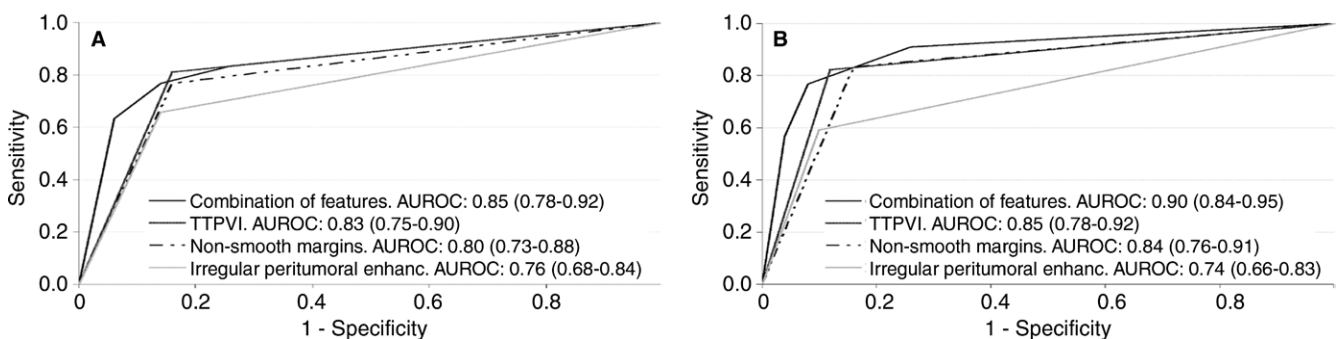
Figure 4

Figure 4: AUROCs of each radiologic feature and of the sum of features for, *A,* observer 1 and, *B,* observer 2. The 95% confidence intervals for each AUROC are reported in parentheses. For observer 1, the AUROC of the sum of features was significantly higher than the sole presence of nonsmooth tumor margins and the presence of irregular peritumoral enhancement ($P = .026$ and $P = .001$, respectively), whereas the magnitude of the difference with TTPVI was not significant ($P = .190$). For observer 2, the AUROC of the sum of features was significantly higher than that for the three single radiologic features: nonsmooth tumor margins, $P = .012$; presence of irregular peritumoral enhancement, $P = .001$; and TTPVI, $P = .032$.

Table 4

Accuracy of Radiologic Features of HCC in Relationship to Presence of MVI

Tumor Sizes and No. of "Worrisome" Radiologic Features	Observer 1		Observer 2	
	No. of Nodules	Predictive Values	No. of Nodules	Predictive Values
All tumors				
Zero features (NPV)	52	0.71 (0.59, 0.83)	45	0.82 (0.71, 0.93)
One feature (PPV)	12	0.50 (0.22, 0.78)	22	0.59 (0.39, 0.80)
Two features (PPV)	16	0.75 (0.54, 0.96)	20	0.90 (0.77, 1.00)
Three features (PPV)	60	0.95 (0.89, 1.00)	53	0.96 (0.91, 1.00)
AUROC	140	0.85 (0.78, 0.92)	140	0.90 (0.84, 0.95)
Tumors < 2 cm				
Zero features (NPV)	25	0.84 (0.69, 0.98)	23	0.91 (0.79, 1.00)
One feature (PPV)	5	0.40 (0.00, 0.83)	7	0.43 (0.06, 0.80)
Two features (PPV)	3	0.67 (0.13, 1.00)	3	1.00 (NC)
Three features (PPV)	4	1.00 (NC)	4	1.00 (NC)
AUROC	37	0.78 (0.62, 0.94)	37	0.86 (0.73, 0.99)
Tumors 2–5 cm				
Zero features (NPV)	18	0.61 (0.39, 0.84)	15	0.73 (0.50, 0.96)
One feature (PPV)	5	0.60 (0.17, 1.00)	11	0.64 (0.35, 0.92)
Two features (PPV)	9	0.67 (0.36, 0.97)	10	0.80 (0.55, 1.00)
Three features (PPV)	30	0.93 (0.84, 1.00)	26	0.96 (0.89, 1.00)
AUROC	62	0.80 (0.69, 0.91)	62	0.87 (0.74, 0.94)
Tumors > 5 cm				
Zero features (NPV)	9	0.56 (0.23, 0.88)	7	0.71 (0.38, 1.00)
One feature (PPV)	2	0.50 (0.19, 1.00)	4	0.75 (0.32, 1.00)
Two features (PPV)	4	1.00 (NC)	7	1.00 (NC)
Three features (PPV)	26	0.96 (0.88, 1.00)	23	0.96 (0.87, 1.00)
AUROC	41	0.84 (0.67, 1.00)	41	0.88 (0.67, 1.00)

Note.—Numbers in parentheses are 95% confidence intervals. NC = not computable, NPV = negative predictive value, PPV = positive predictive value.

at CT hepatic arteriography and CT arterioportography. All these authors used imaging techniques not commonly used in Western countries and not included in the AASLD guidelines (1). Our data suggest that it is possible to assess peritumoral enhancement by using noninvasive techniques, such as CT or dynamic MR imaging, which are recommended for HCC diagnosis (1).

Specific imaging features on CT images that are highly predictive for MVI were previously identified by Segal et al (20), who called TTPVI "internal arteries" and "hypodense halos." These are systematically and univocally correlated to a specific HCC molecular profile, derived from a venous invasion gene profile associated with angiogenesis, cellular proliferation, and matrix invasion (20). To our knowledge, TTPVI

has not been not externally validated prior to our study, in which we tested TTPVI in a larger population, studied with both CT and MR imaging; our data confirmed a strong association of these imaging features with MVI ($P < .001$ for both observers), having the same diagnostic accuracy for CT and MR imaging investigations. Moreover, for observer 1, TTPVI showed the highest prevalence among HCCs with MVI as compared with the other "worrisome" radiologic features. This triple association between TTPVI, MVI, and the molecular profile may enable the use of imaging to reconstruct the global gene expression programs of HCC in the future, thereby creating a noninvasive molecular portrait of the tumor and instituting personalized targeted therapies.

Large tumor size has historically been considered one of the most reliable predictors of MVI in HCC (28–30). However, there are conflicting data regarding the usefulness of tumor size alone in predicting MVI in HCC. An HCC up to 2 cm has low-grade malignancy on the basis of the so-called stepwise progression hypothesis (28,31), but cases of HCC up to 2 cm have been described with MVI and a poor prognosis on the basis of the alternative hypothesis of de novo development (32). Furthermore, patients with an HCC larger than 10 cm without MVI have been reported to have a prognosis similar to those with an HCC smaller than 5 cm without MVI after hepatic resection (33).

In our study, large tumor size was significantly related to more frequent MVI, which is different from what was reported by Chandarana et al (11). This is probably due to selection bias; nearly all the patients with HCC in that study met the Milan criteria, with a mean tumor size of 2.3 cm (range, 0.5–6.1 cm) (11), whereas we enrolled patients who had undergone hepatic resection with larger tumors (30% of cases had an HCC > 5 cm).

Because of these conflicting data regarding the usefulness of tumor size alone in predicting MVI, in our study, we evaluated the diagnostic accuracy of nonsmooth tumor margins, peritumoral enhancement, and TTPVI in predicting MVI alone and in combination in three nodule dimension groups: smaller than 2 cm, 2–5 cm, and larger than 5 cm. It was noted that our imaging parameters were a function of tumor size in predicting MVI—that is, the negative predictive value of the absence of radiologic features decreased with increasing nodule size, meaning that these features can be more useful in smaller nodules, whereas for large tumors, size had a greater weight in predicting MVI. However, we observed that the presence of the three "worrisome" radiologic features had a positive predictive value (above 0.90) independent of tumor size, with no significant interobserver differences. This last figure, the simultaneous presence of the

three radiologic features (nonsmooth tumor margins, peritumoral enhancement, and TTPVI), which was strongly predictive of MVI in HCC regardless of tumor size, could be extremely important. First, the widespread use of screening programs could help in the identification of small tumors in which MVI could be assessed, regardless of size. For the most part, this result could allow identification of patients with MVI in the pretreatment stage, opening new scenarios for choosing among treatments considered curative, such as liver transplantation, hepatic resection, and ablation, and those considered palliative, such as transarterial chemoembolization or radioembolization. Furthermore, a change in the surgical strategy for patients with MVI could be suggested by using a more aggressive approach. Moreover, in preventing HCC recurrences after ablation, occurring with rates similar to those after hepatic resection (3), identification of patients with MVI can also orient toward a more aggressive strategy, with a larger ablated area in combination with adjuvant systemic or intraarterial therapy.

In our study, multinodularity was not significantly related to MVI; however, our results were not completely representative, since our series included, for the most part, single tumors indicated for hepatic resection (only 8.6% of patients [12 of 140] had more than one HCC). This selection bias could explain the discordancy with the results of Chandarana et al (11), who enrolled patients with more than one tumor in 45% of cases and demonstrated multinodularity as being predictive of MVI.

Our study had a number of limitations. First, the retrospective design of the present study, together with the selection bias of surgical candidates, may result in an incomplete representation of all HCC radiologic features. Another limitation is the single-center study, which is a strong factor in interobserver coherence. Additionally, newer imaging methods, such as diffusion-weighted imaging or hepatobiliary phase gadolinium ethoxybenzyl diethylenetriamine pentaacetic acid MR

imaging, were not evaluated, since it was decided to test the "worrisome" features by using the imaging techniques recommended by the AASLD guidelines for HCC diagnosis (1).

In conclusion, some "worrisome" imaging features, such as nonsmooth tumor margins, peritumoral enhancement, TTPVI ("internal arteries" and "hypoattenuating halos"), and large tumor size, were significant predictors of the presence of MVI in HCC. Furthermore, the simultaneous nodule positivity with the three "worrisome" radiologic features of nonsmooth tumor margins, peritumoral enhancement, and TTPVI has a high positive predictive value in the prediction of MVI, independent of tumor size. These results were obtained by using CT and MR imaging, the imaging techniques recommended for HCC diagnosis. Our data might play an important role in the present and future management of HCC by identifying MVI-positive patients during the decision-making stage for appropriate therapy. It is necessary to design studies to establish the best therapy for imaging patients with MVI. By doing so, we would be able to perform more appropriate patient selection, adopt a more aggressive surgical and/or ablative approach, and use different techniques for treating recurrences in patients with MVI.

References

1. Forner A, Llovet JM, Bruix J. Hepatocellular carcinoma. Lancet 2012;379(9822):1245–1255.

2. Zimmerman MA, Ghobrial RM, Tong MJ, et al. Recurrence of hepatocellular carcinoma following liver transplantation: a review of preoperative and postoperative prognostic indicators. Arch Surg 2008;143(2):182–188; discussion 188.

3. Bruix J, Gores GJ, Mazzaferro V. Hepatocellular carcinoma: clinical frontiers and perspectives. Gut 2014;63(5):844–855.

4. Llovet JM, Schwartz M, Mazzaferro V. Resection and liver transplantation for hepatocellular carcinoma. Semin Liver Dis 2005;25(2):181–200.

5. Roayaie S, Blume IN, Thung SN, et al. A system of classifying microvascular invasion to predict outcome after resection in patients with hepatocellular carcinoma. Gastroenterology 2009;137(3):850–855.

6. Miyata R, Tanimoto A, Wakabayashi G, et al. Accuracy of preoperative prediction of microinvasion of portal vein in hepatocellular carcinoma using superparamagnetic iron oxide–enhanced magnetic resonance imaging and computed tomography during hepatic angiography. J Gastroenterol 2006;41(10):987–995.

7. Cucchetti A, Piscaglia F, Frigioni AD, et al. Preoperative prediction of hepatocellular carcinoma tumour grade and microvascular invasion by means of artificial neural network: a pilot study. J Hepatol 2010;52(6):880–888.

8. Hirokawa F, Hayashi M, Miyamoto Y, et al. Outcomes and predictors of microvascular invasion of solitary hepatocellular carcinoma. Hepatol Res 2014;44(8):846–853.

9. Pawlik TM, Gleisner AL, Anders RA, Assumpcao L, Maley W, Choti MA. Preoperative assessment of hepatocellular carcinoma tumor grade using needle biopsy: implications for transplant eligibility. Ann Surg 2007;245(3):435–442.

10. Rodríguez-Perálvarez M, Luong TV, Andreana L, Meyer T, Dhillon AP, Burroughs AK. A systematic review of microvascular invasion in hepatocellular carcinoma: diagnostic and prognostic variability. Ann Surg Oncol 2013;20(1):325–339.

11. Chandarana H, Robinson E, Hajdu CH, Drozhinin L, Babb JS, Taouli B. Microvascular invasion in hepatocellular carcinoma: is it predictable with pretransplant MRI? AJR Am J Roentgenol 2011;196(5):1083–1089.

12. D'Amico F, Schwartz M, Vitale A, et al. Predicting recurrence after liver transplantation in patients with hepatocellular carcinoma exceeding the up-to-seven criteria. Liver Transpl 2009;15(10):1278–1287.

13. Lim KC, Chow PK, Allen JC, et al. Microvascular invasion is a better predictor of tumor recurrence and overall survival following surgical resection for hepatocellular carcinoma compared to the Milan criteria. Ann Surg 2011;254(1):108–113.

14. Gouw AS, Balabaud C, Kusano H, Todo S, Ichida T, Kojiro M. Markers for microvascular invasion in hepatocellular carci-

noma: where do we stand? Liver Transpl 2011;17(17 Suppl 2):S72–S80.

15. Fukuda S, Itamoto T, Nakahara H, et al. Clinicopathologic features and prognostic factors of resected solitary small-sized hepatocellular carcinoma. Hepatogastroenterology 2005;52(64):1163–1167.

16. Shindoh J, Andreou A, Aloia TA, et al. Microvascular invasion does not predict long-term survival in hepatocellular carcinoma up to 2 cm: reappraisal of the staging system for solitary tumors. Ann Surg Oncol 2013;20(4):1223–1229.

17. Eguchi S, Takatsuki M, Hidaka M, et al. Predictor for histological microvascular invasion of hepatocellular carcinoma: a lesson from 229 consecutive cases of curative liver resection. World J Surg 2010;34(5):1034–1038.

18. Chou CT, Chen RC, Lee CW, Ko CJ, Wu HK, Chen YL. Prediction of microvascular invasion of hepatocellular carcinoma by pre-operative CT imaging. Br J Radiol 2012;85(1014):778–783.

19. Chou CT, Chen RC, Lin WC, Ko CJ, Chen CB, Chen YL. Prediction of microvascular invasion of hepatocellular carcinoma: preoperative CT and histopathologic correlation. AJR Am J Roentgenol 2014;203(3):W253–W259.

20. Segal E, Sirlin CB, Ooi C, et al. Decoding global gene expression programs in liver cancer by noninvasive imaging. Nat Biotechnol 2007;25(6):675–680.

21. Bruix J, Sherman M; Practice Guidelines Committee, American Association for the Study of Liver Diseases. Management of hepatocellular carcinoma. Hepatology 2005;42(5):1208–1236.

22. Bruix J, Sherman M; American Association for the Study of Liver Diseases. Management of hepatocellular carcinoma: an update. Hepatology 2011;53(3):1020–1022.

23. Cucchetti A, Ercolani G, Vivarelli M, et al. Is portal hypertension a contraindication to hepatic resection? Ann Surg 2009;250(6):922–928.

24. Vitale A, Morales RR, Zanus G, et al. Barcelona Clinic Liver Cancer staging and transplant survival benefit for patients with hepatocellular carcinoma: a multicentre, cohort study. Lancet Oncol 2011;12(7):654–662.

25. Kim H, Park MS, Choi JY, et al. Can microvessel invasion of hepatocellular carcinoma be predicted by pre-operative MRI? Eur Radiol 2009;19(7):1744–1751.

26. Nishie A, Yoshimitsu K, Asayama Y, et al. Radiologic detectability of minute portal venous invasion in hepatocellular carcinoma. AJR Am J Roentgenol 2008;190(1):81–87.

27. Matsui O, Kobayashi S, Sanada J, et al. Hepatocelluar nodules in liver cirrhosis: hemodynamic evaluation (angiography-assisted CT) with special reference to multistep hepatocarcinogenesis. Abdom Imaging 2011;36(3):264–272.

28. Pawlik TM, Delman KA, Vauthey JN, et al. Tumor size predicts vascular invasion and histologic grade: Implications for selection of surgical treatment for hepatocellular carcinoma. Liver Transpl 2005;11(9):1086–1092.

29. Taketomi A, Sanefuji K, Soejima Y, et al. Impact of des-gamma-carboxy prothrombin and tumor size on the recurrence of hepatocellular carcinoma after living donor liver transplantation. Transplantation 2009;87(4):531–537.

30. Kim SJ, Lee KK, Kim DG. Tumor size predicts the biological behavior and influence of operative modalities in hepatocellular carcinoma. Hepatogastroenterology 2010;57(97):121–126.

31. Sakamoto M, Hirohashi S, Shimosato Y. Early stages of multistep hepatocarcinogenesis: adenomatous hyperplasia and early hepatocellular carcinoma. Hum Pathol 1991;22(2):172–178.

32. Theise ND, Marcelin K, Goldfischer M, Hytiroglou P, Ferrell L, Thung SN. Low proliferative activity in macroregenerative nodules: evidence for an alternate hypothesis concerning human hepatocarcinogenesis. Liver 1996;16(2):134–139.

33. Choi GH, Han DH, Kim DH, et al. Outcome after curative resection for a huge (≥10 cm) hepatocellular carcinoma and prognostic significance of gross tumor classification. Am J Surg 2009;198(5):693–701.